JACS
JOURNAL OF THE AMERICAN CHEMICAL SOCIETY
pubs.acs.org/JACS
Communication

Direct Observation of All Open-Shell Intermediates in a Photocatalytic Cycle

Jian-Qing Qi,‡ Weiqun Suo,‡ Jing Liu, Songtao Sun, Lei Jiao,* and Xingwei Guo*

Cite This: J. Am. Chem. Soc. 2024, 146, 7140−7145
Read Online
ACCESS | Metrics & More | Article Recommendations | Supporting Information

ABSTRACT: Molecular photocatalysis has shown tremendous success in sustainable energy and chemical synthesis. However, visualizing the transient open-shell intermediates in photocatalysis is a significant and long-standing challenge. By employing our recently developed innovative time-resolved electron paramagnetic resonance technique, we directly observed all radicals and radical ions involved in the photocatalytic addition of pempidine to *tert*−butyl acrylate. The full picture of the photocatalytic cycle is vividly illustrated by the fine structures, chemical kinetics, and dynamic spin polarization of all open-shell intermediates directly observed in this prototypical system. Given the universality of this methodology, we believe it greatly empowers the research paradigm of direct observation in both photocatalysis and radical chemistry.

The ability to directly "watch" the evolution of radical intermediates in a photocatalytic reaction has long been a coveted goal for many chemists. Over the past decades, transient absorption (TA) and time-resolved electron paramagnetic resonance (TREPR) spectroscopy have been used in studying transient radical species,[1−12] which offered valuable mechanistic insights into many elementary radical reactions. However, transient spectroscopic methods encounter significant difficulties in elucidating the structures of the short-lived species. Meanwhile, the current TREPR technique suffers from inherent low sensitivity and limited observation time window depending on the time domain of hyperpolarization,[6,13] thereby making it incapable of observing full reaction cascades. To date, direct observation of a photocatalytic cycle with unambiguous characterization and tracking of all radical intermediates remains unprecedented. This highlights the pressing need for an advanced time-resolved spectroscopic method that provides both fine structural information and exceptional sensitivity.

We have recently invented a new EPR technique, which we named the ultrawide single sideband phase-sensitive detection (U-PSD) TREPR (Figure 1A).[14] By employing this technique, we could accurately retrieve a transient EPR signal, which results in first-derivative EPR spectra with both high time-resolution and exceptional sensitivity. This advancement enables the detection of weak signals of transient radicals in a solution-phase chemical reaction over a wide time range, which was previously not possible with existing TREPR techniques. Herein, we present the first direct observation of all open-shell intermediates in a full photocatalytic cycle using this technique, which provides mechanistic insights into the photocatalytic radical reaction with an unprecedented level of detail.

We focused on a representative photocatalytic reaction, the addition of amine α-C−H bonds to alkenes promoted by visible light,[15] which can be catalyzed by several photoredox catalysts (Figure 1B). As a model, the reaction of pempidine (*N*,2,2,6,6-pentamethylpiperidine, PMP) with *tert*-butyl acrylate (**1**) under visible light (450 nm) catalyzed by either an iridium-based photocatalyst $[Ir(dF\text{-}CF_3\text{-}ppy)_2(dtbbpy)]PF_6$ (**PC1**) or an organic photocatalyst 1,2,3,5-tetrakis(carbazol-9-yl)-4,6-dicyanobenzene (4CzIPN, **PC2**) afforded Giese-type adduct **2** in good yields (Table S1). This reaction is believed to proceed through a typical redox-neutral photocatalytic cycle involving elementary steps of single-electron oxidation, proton transfer, radical addition, and single-electron reduction,[15] with the formation of three key radical intermediates **R1•** to **R3•** (Figure 1C). Although this catalytic cycle has been commonly proposed previously, it has never been directly observed experimentally.

The measurements were done by flowing an acetonitrile solution of PMP, **1**, the photocatalyst, and 4-dimethylaminopyridine (DMAP) through the resonator of the spectrometer while applying repeated laser pulses at 298 K. In the reaction catalyzed by **PC1**, three radical species were identified in different time regions. These species have been unambiguously identified as amine radical cation (**R1•**), α-aminoalkyl radical (**R2•**), and radical adduct (**R3•**), which was achieved by analyzing the structural information (Figures S2−S4), specifically the hyperfine splittings (HFSs), extracted from well-resolved TREPR spectra (Figure 1D). It is notable that the acquired TREPR spectra exhibited a hyperpolarized pattern, which provided key information for the single-electron transfer (SET) steps (*vide infra*).

The kinetic profiles of these species were determined by monitoring nonoverlapping EPR peaks (Figure 1E, left). The

Received: December 20, 2023
Revised: January 28, 2024
Accepted: March 7, 2024
Published: March 11, 2024

https://doi.org/10.1021/jacs.3c14471
J. Am. Chem. Soc. 2024, 146, 7140−7145

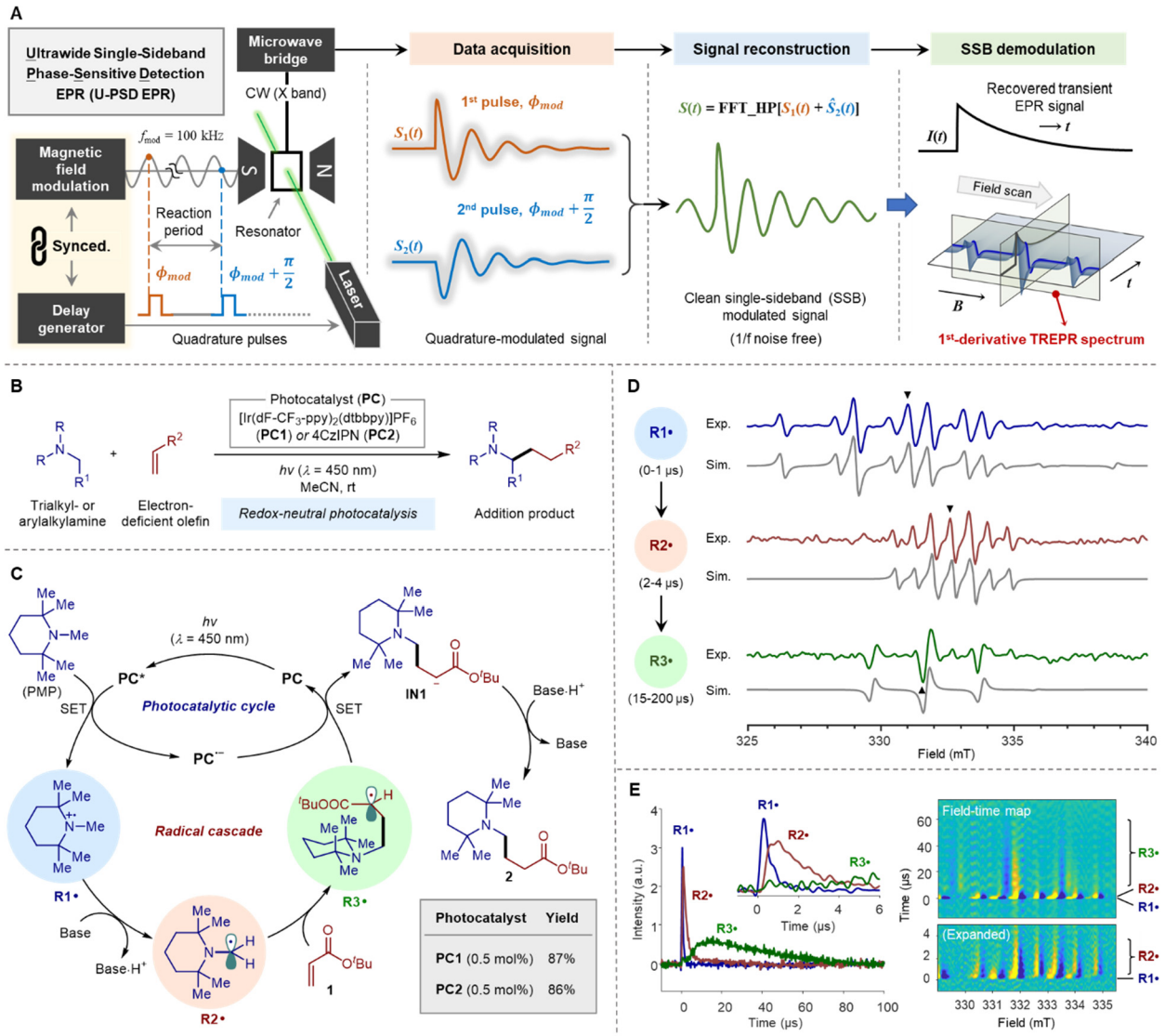

Figure 1. Direct observation of a photocatalytic cycle with the U-PSD EPR. (A) Schematic of the U-PSD EPR technique. (B) General reaction of photocatalyzed addition of amines to olefins. (C) Proposed mechanism for the reaction between pempidine and *tert*-butyl acrylate. (D) TREPR spectra of three radical intermediates (X-band, 9.33 GHz). Peaks marked with black triangles were used for acquiring kinetic profiles. (E) Kinetic traces of the radicals involved and a field-time map of the reaction.

kinetic plots indicated the sequential formation of **R1•**, **R2•**, and **R3•** with distinct lifetimes in the reaction system. This aligns well with the proposed reaction pathway of **R1•** → **R2•** → **R3•**. Observed kinetic traces provide valuable information about the lifetime of these radicals, as well as their spin dynamics (Figure S5). A field-time map constructed using acquired TREPR data exhibited the panorama of the evolution of radical intermediates over the reaction time course (Figure 1E, right; see Figure S6 for details).

In addition to identifying and tracing all radical intermediates, we were able to acquire more detailed information about each individual step. We then focused on the initial SET step of the radical cascade, which resulted in the formation of amine cation radical **R1•** through photoinduced SET between PMP and **PC1** or **PC2** (Figure 2A). The measurements were done using a simplified reaction system only consisting of PMP and the photocatalyst. The TREPR spectra acquired by integrating 0−2 μs after the laser pulse (Figure 2B, red and blue spectra) confirmed the formation of the same radical intermediate with different photocatalysts, as identical splitting pattern were observed. The simulated steady-state EPR spectrum of **R1•** (Figure 2B, black spectrum) revealed HFSs from ^{14}N and α-C−H (a_N = 2.05 mT, $3a_H$ = 2.76 mT), which are in agreement with previously reported data for similar alkyl amine radical cations.[16] The value of a_N close to 2.0 mT suggests a planar geometry at the nitrogen atom in this radical cation.[17]

It is important to note that the experimental TREPR spectra of **R1•** generated with photocatalysts **PC1** (Figure 2B, red spectrum) and **PC2** (Figure 2B, blue spectrum) exhibited significant extent of hyperpolarization due to chemically induced dynamic electron polarization (CIDEP).[16] Interestingly, the polarization center of the two spectra matched the spectral centers of the reduced form of photocatalysts (g = 1.9875 and 2.0034 for **PC1**$^{\bullet-}$ and **PC2**$^{\bullet-}$, respectively; see Figure S8). This observation indicates that radical cation **R1•** originates from the geminate radical pairs generated by excited-state SET, which provides direct evidence for the electron

https://doi.org/10.1021/jacs.3c14471
J. Am. Chem. Soc. 2024, 146, 7140−7145

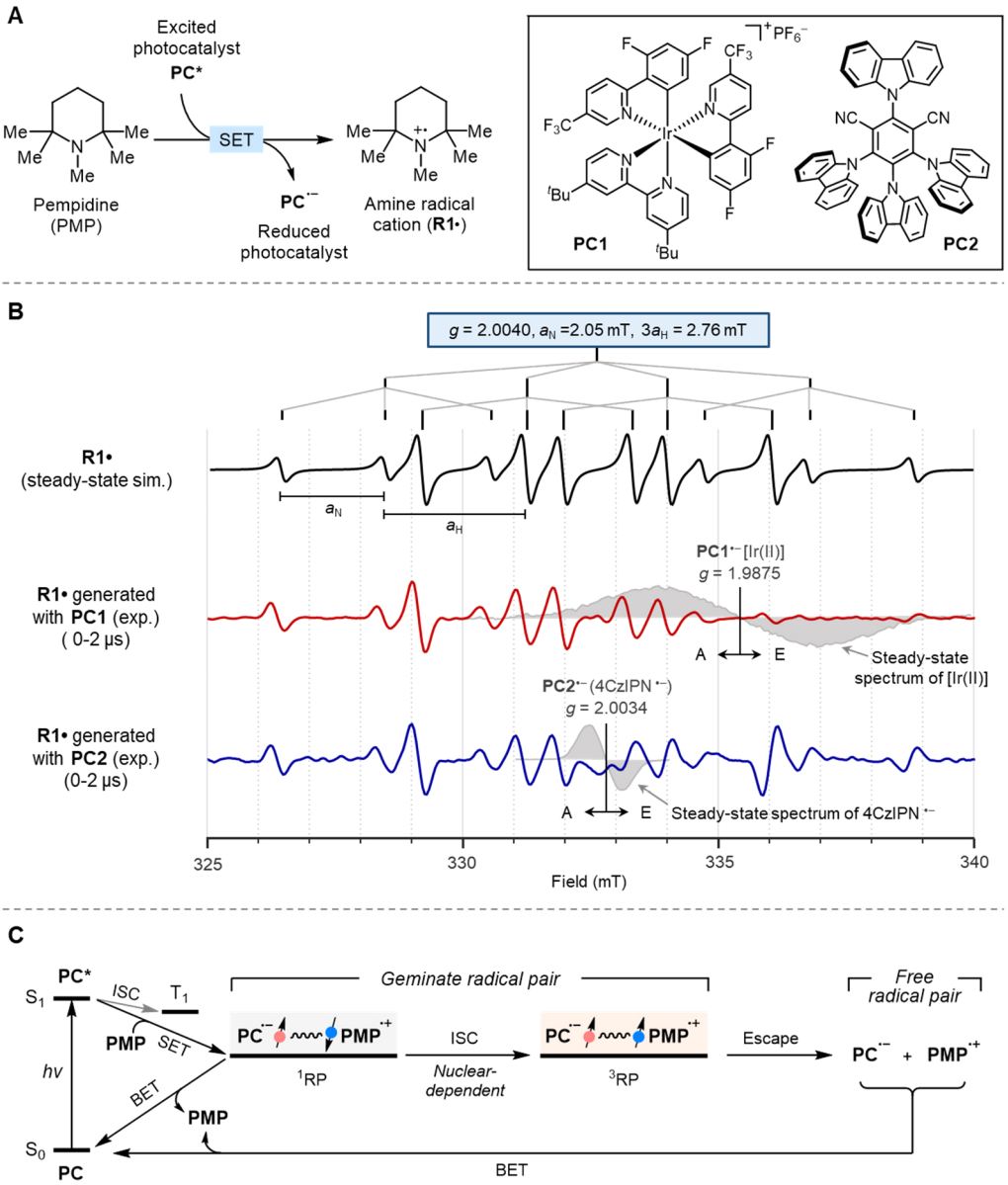

Figure 2. Observing the SET between pempidine and the excited photocatalyst. (A) Photoinduced SET reaction. (B) EPR spectra of **R1•** (black, simulated steady-state spectrum) generated with **PC1** (red) and **PC2** (blue). (C) Geminate radical pair mechanism of the photoinduced SET.

transfer step (Figure 2C). Remarkably, the observed absorption/emission (A/E)-type polarization pattern in both cases (see Figure S7 for detailed analysis) indicates that photoinduced SET with both photocatalysts occurs through the formation of an initial singlet radical pair (^{1}RP)[18−20] supported by a triplet quenching experiment (Figure S15). Thus, the singlet excited states of both [Ir(dF-CF$_3$-ppy)$_2$(dtbbpy)]PF$_6$ and 4CzIPN had a significant contribution to their photoredox activity in this reaction, which is in line with a recent study on the photoinduced SET between 4CzIPN and azide anion.[11] This observation offers explicit information for the state of the excited photocatalyst involved in the SET process.

The amine radical cation is believed to be a highly active intermediate. With the help of the U-PSD EPR technique, we could elucidate the reactivity of the amine radical cation **R1•** through clear experimental evidence (Figure 3A).

We performed a study on the reaction between PMP and **PC1** in the presence of different concentrations of DMAP as the base. Without an external base, **R1•** was found to be the major radical species observed in the TREPR spectrum (Figure 3B, red spectrum). However, upon addition of DMAP, a new radical species started to appear while **R1•** was disappearing (Figure 3B, blue spectrum). This new radical species was assigned as α-aminoalkyl radical **R2•** on the basis of its spectral characteristics. It was found that higher concentrations of DMAP resulted in a higher degree of conversion of **R1•** to **R2•** within the same time period (Figure 3B, green spectrum). This observation indicates that the formation of **R2•** from **R1•** involves a deprotonation process and that DMAP is a more efficient base than PMP itself.

The spectral signature of **R2•** (Figure 3B) indicates the HFS from both ^{14}N and α-C−H (a_N = 0.71 mT, $2a_H$ = −1.42 mT), which align with previously documented values of α-aminoalkyl radicals.[21] Compared with the coupling constant in methyl radical ($3a_H$ = −2.30 mT), the smaller amplitude from α−C-H of **R2•** suggests a pyramidalization of the α-

https://doi.org/10.1021/jacs.3c14471
J. Am. Chem. Soc. 2024, 146, 7140−7145

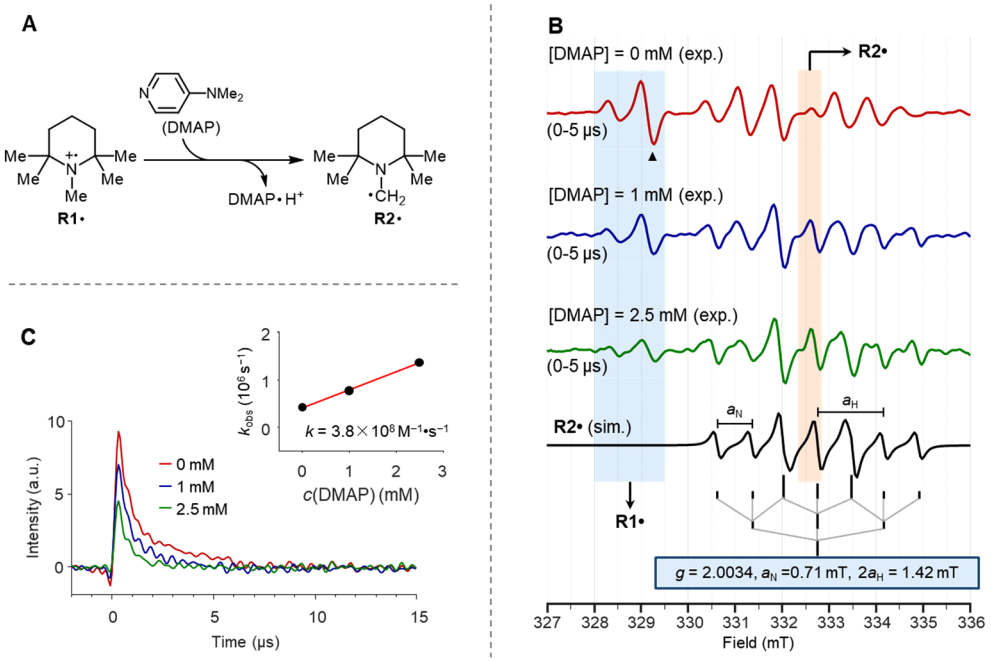

Figure 3. Observing the formation of radical **R2•**. (A) Deprotonation reaction of **R1•**. (B) TREPR spectra with different DMAP concentrations. The peak marked with a black triangle was used for kinetic profiles. (C) Kinetic profiles of **R1•** with different DMAP concentrations.

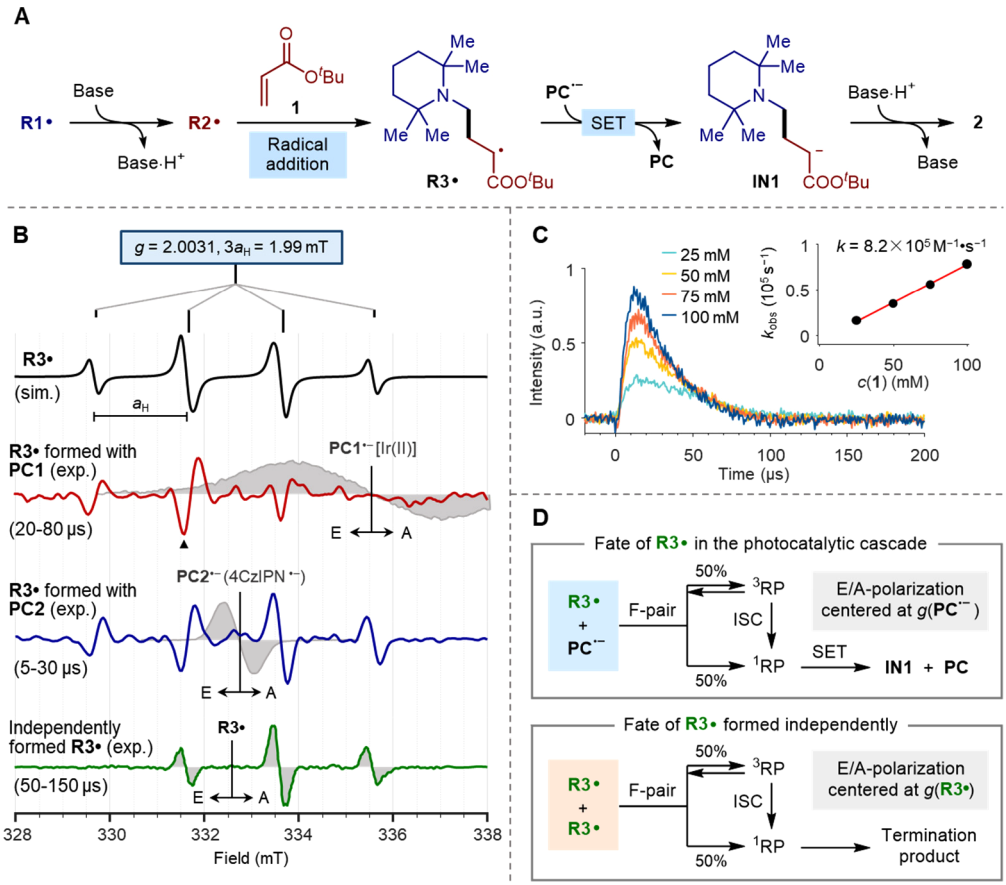

Figure 4. Observing radical addition and subsequent SET reduction steps. (A) Reaction cascade from **R1•** to the final product. (B) TREPR spectra of radical **R3•**: black (simulated steady-state spectrum), red (generated with **PC1**), blue (generated with **PC2**), and green (generated without a photocatalyst). The peak marked with a black triangle was monitored to acquire the kinetic profiles. (C) Kinetic profiles of **R3•** with different concentrations of *tert*-butyl acrylate. (D) Schematic of the polarization mechanism of **R3•**.

https://doi.org/10.1021/jacs.3c14471
J. Am. Chem. Soc. 2024, 146, 7140−7145

aminoradical center,[17] and the HFS of ^{14}N originates from spin delocalization.

For this deprotonation step, we not only observed the spectroscopic change but also acquired its kinetics by tracing the decay of **R1•** (Figure 3C) and the formation of **R2•** (Figure S9). As the concentration of base increased, the decay of **R1•** became faster, which corresponded to the decrease in build-up intensity of the cation radical **R1•**. By fitting the kinetic traces of this series, the second-order rate constant for the proton transfer step was determined to be 3.8×10^8 M^{-1} s^{-1} (Figure 3C, inset; see Figure S13 and Table S2 for details), which accounted for the expected high reactivity of the amine radical cation. To the best of our knowledge, the transformation of amine radical cation to α-aminoalkyl radical has never been observed in such level of detail.[22]

To further investigate the fate of the α-aminoalkyl radical **R2•** (Figure 4A), we conducted TREPR measurements for the reaction system consisting of PMP, DMAP, acceptor **1**, and different photocatalysts. With both **PC1** and **PC2**, the same radical intermediate was observed in carefully time-gated TREPR spectra to observe the late stage of the reaction (Figure 4B, red and blue spectra). In order to identify the nature of the observed radical, we performed an additional experiment involving the reaction between PMP, di-*tert*-butylperoxide (DTBP), and **1** to independently generate the radical intermediate under nonphotocatalytic conditions[23] (see Figure S10 for details). The acquired spectrum confirmed the formation of the identical radical intermediate assigned as radical adduct **R3•** (Figure 4B, green spectrum). This radical exhibits degenerated hyperfine splitting from α- and β-C−H ($3a_H = -1.99$ mT), as revealed by the simulated steady-state EPR spectrum (Figure 4B, gray; see Figures S4, S11, S12 for details), which is inconsistent with previously reported data for α-carbonyl radicals.[24,25]

By monitoring the designated peak corresponding to radical adduct **R3•** in the PMP/DMAP/**1**/**PC1** reaction system with varying concentrations of acceptor **1**, we observed concentration-dependent changes in the kinetic profile of this radical intermediate (Figure 4C). Nonlinear fitting of the acquired kinetic data allowed us to obtain the second-order rate constant of 8.2×10^5 M^{-1} s^{-1} for the radical addition (Figure 4C, inset; see Figure S14 and Table S3 for details), which is consistent with the magnitudes of the reported rate constants for the addition of α-aminoalkyl radicals to methyl acrylate.[23]

The remaining puzzle of the whole photocatalytic cycle is the reaction pathway of **R3•**, specifically how this radical transforms into the final product. It is believed that this step proceeds through an SET reduction/protonation process, supported by the redox potentials of **R3•** and **PC**$^{\bullet-}$.[26−28] Additionally, another viable pathway involves hydrogen atom transfer (HAT) from the amine α-C−H bond, considering the bond dissociation energies.[29,30] However, because of the lack of direct experimental evidence, the mechanism of this step remains an unanswered question.

Looking into the TREPR spectra of **R3•** formed with **PC1** and **PC2**, we found that the observed E/A-type polarization fits the spectral centers of the reduced form of photocatalysts, Ir(II) and 4CzIPN$^{\bullet-}$, respectively (Figure 4B, red and blue spectra). This is in line with a characteristic free radical pair (F-pair) CIDEP mechanism (Figure 4D, top), which discloses the interaction between **R3•** and **PC**$^{\bullet-}$.[19] This clearly supported the SET reduction pathway in the present reaction. By comparison, we found that independently formed **R3•** in the absence of reduced photocatalyst exhibited E/A-type polarization with a different center (Figure 4B, green spectrum), which fits into a scenario of F-pair CIDEP caused by self-termination[19] of **R3•** (Figure 4D, bottom). The polarization pattern of the TREPR spectra served as an important probe for elucidating the mechanism of the SET process.

In summary, this study demonstrates the U-PSD EPR technique as a powerful tool for elucidating the mechanistic complexity of radical transformations. It enables direct observation of a full photocatalytic cycle by providing fine structure, kinetics, and spin dynamics of each radical intermediate. We believe that this research has the potential to make a significant impact in the field of radical research.

■ ASSOCIATED CONTENT

Supporting Information

The Supporting Information is available free of charge at https://pubs.acs.org/doi/10.1021/jacs.3c14471.

Details for experimental procedures, spectra simulation, kinetic fitting, and compound characterization (PDF)

■ AUTHOR INFORMATION

Corresponding Authors

Lei Jiao − *Center of Basic Molecular Science (CBMS), Department of Chemistry, Tsinghua University, Beijing 100084, China;* orcid.org/0000-0002-8465-1358; Email: leijiao@mail.tsinghua.edu.cn

Xingwei Guo − *Center of Basic Molecular Science (CBMS), Department of Chemistry, Tsinghua University, Beijing 100084, China;* orcid.org/0000-0002-5461-0360; Email: xingwei_guo@mail.tsinghua.edu.cn

Authors

Jian-Qing Qi − *Center of Basic Molecular Science (CBMS), Department of Chemistry, Tsinghua University, Beijing 100084, China;* orcid.org/0000-0001-5042-6315

Weiqun Suo − *Center of Basic Molecular Science (CBMS), Department of Chemistry, Tsinghua University, Beijing 100084, China*

Jing Liu − *Center of Basic Molecular Science (CBMS), Department of Chemistry, Tsinghua University, Beijing 100084, China*

Songtao Sun − *Center of Basic Molecular Science (CBMS), Department of Chemistry, Tsinghua University, Beijing 100084, China*

Complete contact information is available at: https://pubs.acs.org/10.1021/jacs.3c14471

Author Contributions

‡J.-Q.Q. and W.S. contributed equally.

Funding

This work was supported by Tsinghua University Dushi Program. The National Natural Science Foundation of China (Grant No. 22193011) is acknowledged for financial support.

Notes

The authors declare no competing financial interest.

■ ACKNOWLEDGMENTS

The authors thank Prof. H. Mayr for proofreading the manuscript and Profs. M.-T. Zhang and J. Yang for helpful discussions.

■ ABBREVIATIONS

EPR, electron paramagnetic resonance; TREPR, time-resolved electron paramagnetic resonance; exp., experimental; sim., simulated; ISC, internal system crossing; BET, back electron transfer; RP, radical pair; SET, single-electron transfer

■ REFERENCES

(1) Ishii, K.; Hirose, Y.; Fujitsuka, H.; Ito, O.; Kobayashi, N. Time-Resolved EPR, Fluorescence, and Transient Absorption Studies on Phthalocyaninatosilicon Covalently Linked to One or Two TEMPO Radicals. *J. Am. Chem. Soc.* **2001**, *123* (4), 702−708.

(2) Ahn, J. M.; Ratani, T. S.; Hannoun, K. I.; Fu, G. C.; Peters, J. C. Photoinduced, Copper-Catalyzed Alkylation of Amines: A Mechanistic Study of the Cross-Coupling of Carbazole with Alkyl Bromides. *J. Am. Chem. Soc.* **2017**, *139* (36), 12716−12723.

(3) Sreekanth, R.; Prasanthkumar, K. P.; Sunil Paul, M. M.; Aravind, U. K.; Aravindakumar, C. T. Oxidation Reactions of 1- and 2-Naphthols: An Experimental and Theoretical Study. *J. Phys. Chem. A* **2013**, *117* (44), 11261−11270.

(4) Qin, Y.; Sun, R.; Gianoulis, N. P.; Nocera, D. G. Photoredox Nickel-Catalyzed C-S Cross-Coupling: Mechanism, Kinetics, and Generalization. *J. Am. Chem. Soc.* **2021**, *143* (4), 2005−2015.

(5) Colvin, M. T.; Ricks, A. B.; Scott, A. M.; Smeigh, A. L.; Carmieli, R.; Miura, T.; Wasielewski, M. R. Magnetic Field-Induced Switching of the Radical-Pair Intersystem Crossing Mechanism in a Donor-Bridge-Acceptor Molecule for Artificial Photosynthesis. *J. Am. Chem. Soc.* **2011**, *133* (5), 1240−1243.

(6) Forbes, M. D. E.; Jarocha, L. E.; Sim, S.; Tarasov, V. F. Chapter One - Time-Resolved Electron Paramagnetic Resonance Spectroscopy: History, Technique, and Application to Supramolecular and Macromolecular Chemistry. In *Adv. Phys. Org. Chem.*, Vol. *47*; Williams, I. H.; Williams, N. H., Eds.; Academic Press, 2013; pp 1−83.

(7) Turro, N. J.; Kleinman, M. H.; Karatekin, E. Electron Spin Polarization and Time-Resolved Electron Paramagnetic Resonance: Applications to the Paradigms of Molecular and Supramolecular Photochemistry. *Angew. Chem., Int. Ed.* **2000**, *39* (24), 4436−4461.

(8) Lewis-Borrell, L.; Sneha, M.; Clark, I. P.; Fasano, V.; Noble, A.; Aggarwal, V. K.; Orr-Ewing, A. J. Direct Observation of Reactive Intermediates by Time-Resolved Spectroscopy Unravels the Mechanism of a Radical-Induced 1,2-Metalate Rearrangement. *J. Am. Chem. Soc.* **2021**, *143* (41), 17191−17199.

(9) Bhattacherjee, A.; Sneha, M.; Lewis-Borrell, L.; Tau, O.; Clark, I. P.; Orr-Ewing, A. J. Picosecond to Millisecond Tracking of a Photocatalytic Decarboxylation Reaction Provides Direct Mechanistic Insights. *Nat. Commun.* **2019**, *10* (1), 5152.

(10) Greaves, S. J.; Rose, R. A.; Oliver, T. A. A.; Glowacki, D. R.; Ashfold, M. N. R.; Harvey, J. N.; Clark, I. P.; Greetham, G. M.; Parker, A. W.; Towrie, M.; Orr-Ewing, A. J. Vibrationally Quantum-State-Specific Reaction Dynamics of H Atom Abstraction by CN Radical in Solution. *Science* **2011**, *331* (6023), 1423−1426.

(11) Sneha, M.; Thornton, G. L.; Lewis-Borrell, L.; Ryder, A. S. H.; Espley, S. G.; Clark, I. P.; Cresswell, A. J.; Grayson, M. N.; Orr-Ewing, A. J. Photoredox-HAT Catalysis for Primary Amine α-C-H Alkylation: Mechanistic Insight with Transient Absorption Spectroscopy. *ACS Catal.* **2023**, *13* (12), 8004−8013.

(12) Kandoth, N.; Hernández, J. P.; Palomares, E.; Lloret-Fillol, J. Mechanisms of Photoredox Catalysts: The Role of Optical Spectroscopy. *Sustainable Energy Fuels* **2021**, *5* (3), 638−665.

(13) Karunakaran, C.; Balamurugan, M. Chapter Five - Advances in Electron Paramagnetic Resonance. In *Spin Resonance Spectroscopy*; Karunakaran, C., Ed.; Elsevier, 2018; pp 229−280.

(14) Zhang, S.; Zhou, S.; Qi, J.; Jiao, L.; Guo, X. Time-Resolved Electron Paramagnetic Resonance Spectrometer Based on Ultrawide Single-Sideband Phase-Sensitive Detection. *Rev. Sci. Instrum.* **2023**, *94* (8), 084101.

(15) Nakajima, K.; Miyake, Y.; Nishibayashi, Y. Synthetic Utilization of α-Aminoalkyl Radicals and Related Species in Visible Light Photoredox Catalysis. *Acc. Chem. Res.* **2016**, *49* (9), 1946−1956.

(16) Fessenden, R. W.; Neta, P.; Mellon Inst. Sci.. Electron Spin Resonance Spectra of Di- and Trimethylaminium Radicals. *J. Phys. Chem.* **1972**, *76* (20), 2857−2859.

(17) Gerson, F.; Huber, W. Organic Radicals Centered on One, Two, or Three Atoms. In *Electron Spin Resonance Spectroscopy of Organic Radicals*; John Wiley & Sons, 2003; pp 177−180.

(18) Berliner, L. J.; Bagryanskaya, E. Chemically Induced Electron and Nuclear Polarization. In *Multifrequency Electron Paramagnetic Resonance*; John Wiley & Sons, Ltd, 2011; pp 947−992.

(19) Forbes, M. D. E. Time-Resolved (CW) Electron Paramagnetic Resonance Spectroscopy: An Overview of the Technique and Its Use in Organic Photochemistry. *Photochem. Photobiol.* **1997**, *65* (1), 73−81.

(20) Eills, J.; Budker, D.; Cavagnero, S.; Chekmenev, E. Y.; Elliott, S. J.; Jannin, S.; Lesage, A.; Matysik, J.; Meersmann, T.; Prisner, T.; Reimer, J. A.; Yang, H.; Koptyug, I. V. Spin Hyperpolarization in Modern Magnetic Resonance. *Chem. Rev.* **2023**, *123* (4), 1417−1551.

(21) Wood, D. E.; Lloyd, R. V. EPR of Free Radicals in an Adamantane Matrix. I. Aliphatic Aminoalkyl Radicals. *J. Chem. Phys.* **1970**, *53* (10), 3932−3942.

(22) Das, S.; von Sonntag, C. The Oxidation of Trimethylamine by OH Radicals in Aqueous Solution, as Studied by Pulse Radiolysis, ESR, and Product Analysis. The Reactions of the Alkylamine Radical Cation, the Aminoalkyl Radical, and the Protonated Aminoalkyl Radical. *Z. Naturforsch. B* **1986**, *41* (4), 505−513.

(23) Lalevée, J.; Graff, B.; Allonas, X.; Fouassier, J. P. Aminoalkyl Radicals: Direct Observation and Reactivity toward Oxygen, 2,2,6,6-Tetramethylpiperidine-N-Oxyl, and Methyl Acrylate. *J. Phys. Chem. A* **2007**, *111* (30), 6991−6998.

(24) Foster, T.; Klapstein, D.; West, P. R. Restricted Rotation in α-Carbonyl Radicals. *Can. J. Chem.* **1974**, *52* (3), 524−526.

(25) Kubiak, B.; Lehnig, M.; Neumann, W. P.; Pentling, U.; Zarkadis, A. K. Sterically Hindered Free Radicals. Part 20. EPR and ENDOR Spectroscopy of α-Carbonyl Radicals. *J. Chem. Soc. Perkin Trans. 2* **1992**, No. 9, 1443−1447.

(26) Schmittel, M.; Lal, M.; Lal, R.; Röck, M.; Langels, A.; Rappoport, Z.; Basheer, A.; Schlirf, J.; Deiseroth, H.-J.; Flörke, U.; Gescheidt, G. A Comprehensive Picture of the One-Electron Oxidation Chemistry of Enols, Enolates and α-Carbonyl Radicals: Oxidation Potentials and Characterization of Radical Intermediates. *Tetrahedron* **2009**, *65* (52), 10842−10855.

(27) Ladouceur, S.; Fortin, D.; Zysman-Colman, E. Enhanced Luminescent Iridium(III) Complexes Bearing Aryltriazole Cyclometallated Ligands. *Inorg. Chem.* **2011**, *50* (22), 11514−11526.

(28) Swanick, K. N.; Ladouceur, S.; Zysman-Colman, E.; Ding, Z. Correlating Electronic Structures to Electrochemiluminescence of Cationic Ir Complexes. *RSC Adv.* **2013**, *3* (43), 19961−19964.

(29) Laarhoven, L. J. J.; Mulder, P.; Wayner, D. D. M. Determination of Bond Dissociation Enthalpies in Solution by Photoacoustic Calorimetry. *Acc. Chem. Res.* **1999**, *32* (4), 342−349.

(30) Karty, J. M.; Janaway, G. A.; Brauman, J. I. Conformation-Dependent Reaction Thermochemistry: Study of Lactones and Lactone Enolates in the Gas Phase. *J. Am. Chem. Soc.* **2002**, *124* (18), 5213−5221.

https://doi.org/10.1021/jacs.3c14471
J. Am. Chem. Soc. 2024, 146, 7140−7145